microASAR: A SMALL, ROBUST LFM-CW SAR FOR OPERATION ON UAVS AND SMALL AIRCRAFT

Matthew Edwards, David Madsen*, Craig Stringham*, Alex Margulis†, Brandon Wicks†, and David G. Long**

*Brigham Young University, Provo, UT 84602
†Artemis, Inc., Hauppauge, NY 11788

ABSTRACT

The Artemis microASAR is a flexible, robust SAR system built on the successful legacy of the BYU μSAR [1] [2] and other BYU SAR systems [3]. It is an LFM-CW SAR system designed for low-power operation on small, manned aircraft or UAVs. This paper describes the high-level methodology used in designing the microASAR system and contains a description of the hardware specifications. Performance projections are also calculated and presented.

Index Terms— Synthetic aperture radar, CW radar, chirp radar, airborne radar

1. INTRODUCTION

Synthetic aperture radar (SAR) has proven to be a useful tool in a variety of surveillance and remote sensing applications and much work has gone into developing new systems that meet varying needs. The microASAR is a complete, self-contained SAR system that has been designed specifically to be small and lightweight while still being robust and capable. These characteristics make it an ideal SAR system for use on unmanned aerial vehicles (UAVs) and other small aircraft.

Students at Brigham Young University have designed and tested a number of successful SAR systems. Among these is the BYU μSAR – a lightweight, low-power, stripmap SAR system that has been used to collect data on several different platforms ranging from ground-based vehicles to UAVs to small aircraft [1] [2]. Building on this success, the microASAR has been designed in collaboration with Artemis, Inc., to be a much more robust system. The microASAR is also unique because of its capabilities and extensibility which makes it an ideal sensor for many short- to medium-range SAR applications.

This paper outlines the specifications of the microASAR and discusses some of the methodology used in the design of the system. Projected figures of merit and performance statistics are also calculated and presented. A complete microASAR system is in the final stages of assembly and testing.

2. DESIGN OF THE microASAR

The microASAR uses a linear frequency-modulated (LFM) chirp generated by a direct digital synthesizer (DDS) chip. Although the μSAR used a frequency modulation scheme that ramps up then down, with each up-down cycle comprising one pulse repetition, the microASAR's chirp ramps in a single direction only in order to more easily achieve high pulse repetition frequencies (PRFs). The DDS needs a few clock cycles to reset between chirps, which means that while the microASAR is effectively an LFM-CW radar, its transmit waveform is not strictly continuous wave (CW). Nevertheless, the benefits of LFM-CW are realized in this configuration.

By maximizing the pulse length, an LFM-CW system is able to maintain a high SNR while transmitting with a lower peak power than a comparable pulsed SAR. Also, final processing is simplified by performing an analog "dechirping" of the signal in which the received signal is mixed with a copy of the transmitted signal. Since the waveform is an LFM chirp, the difference between the transmitted chirp and a delayed copy of itself is a single frequency. These frequencies correspond directly to the slant-range of the target. Thus, the dechirped signal is a frequency domain representation of the range-compressed SAR image.

The CW scheme does have the side effect of limiting the unambiguous range that can be imaged by the sensor, and thus the altitude at which the aircraft can fly. Since the microASAR is designed for small, low-flying aircraft, this is not a restriction. The system is very flexible, however, and can be configured to transmit pulsed radar signals if needed.

Since a CW SAR system is constantly transmitting, a bistatic configuration with a separate antenna for the receive channel is used to maximize transmit-receive isolation. An undesirable side effect of bistatic, LFM-CW SAR is feedthrough between the transmit and receive antennas. This relatively strong feedthrough component dominates the low end of the dechirped spectrum and must be removed before final processing. It is desirable to remove the feedthrough component as early as possible in order to minimize the required dynamic range at the receiver and analog-to-digital converter (ADC), which would otherwise need to handle both the strong feedthrough and the weak radar returns. Feedthrough removal can be accomplished at baseband by utilizing a high-pass filter with a very low cutoff frequency, but this type of filter generally has a very long impulse response, which leads to degradation of the filtered signal. The microASAR removes the feedthrough component after dechirping with a surface acoustic wave band-pass filter (SAW BPF) centered at 500 MHz. The SAW BPF was selected for this purpose because of its high performance and ready availability. In order to accomplish the feedthrough removal, the frequency of the crystal oscillator, from which all signals are generated, is chosen so that the feedthrough component in the dechirped signal is mixed down to the first null of the BPF. This feedthrough removal scheme is illustrated in Fig. 1.

As seen in Fig. 1, Δf is the frequency difference between the feedthrough component and the return from nadir. We define $k_r = B f_p$ where B is the bandwidth of the LFM chirp and f_p is the PRF. We also define Δt, the time required for a transmitted chirp to travel from the transmitting antenna to a target and back, as $\Delta t = \frac{2R}{c_0}$ where R is the slant range from the antenna to the target and c_0 is the
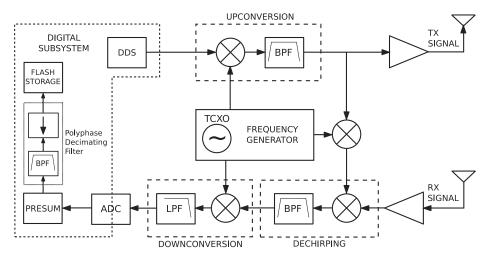
Fig. 2. Simplified block diagram for the microASAR system. All clocks and signals are derived from the temperature compensated crystal oscillator (TCXO).
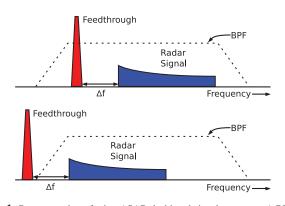

Fig. 1. Representation of microASAR dechirped signal spectrum. A BPF is used to filter the feedthrough component by shifting the spectrum down. Δf is the frequency representation of the distance between the platform and the ground.

speed of light. Then $\Delta f = k_r \Delta t$. We label the Δt's corresponding to feedthrough and nadir Δt_{ft} and Δt_n, respectively. Then,

$$\Delta f_{min} = k_r(\Delta t_n - \Delta t_{ft}) \qquad (1)$$

is the minimum Δf that places the feedthrough component in the null of the BPF while allowing the radar signal to pass through the BPF. Substituting k_r and Δt as defined above yields

$$\Delta f_{min} = \frac{2B f_{p,min}}{c_0}(R_n - \beta) \qquad (2)$$

where R_n is the distance from the antenna to nadir and β is the length of the effective free-space path that the feedthrough signal takes. β is on the order of a few meters or less. Choosing Δf_{min} based on the roll-off of the BPF, the minimum PRF is

$$f_{p,min} = \frac{\Delta f_{min} c_o}{2B(R_n - \beta)} \qquad (3)$$

The frequency difference between the 10 dB point and the first null of the BPF is 1.1 MHz. This is Δf in Eq. (3). We also use the values $B = 120$ MHz, $R_n = 100$ m, and $\beta = 2$ m. This yields a

PRF of $f_{p,min} = 14.03$ kHz. As the altitude is increased, the difference between the feedthrough and the first radar return naturally increases so that the required PRF decreases. At $R_n = 1000$ m, for instance, the required PRF is $f_{p,min} = 1.4$ kHz. In normal SAR systems, the PRF must simply be high enough to avoid aliasing of the Doppler spectrum in slow time. The bandwidth of the Doppler spectrum is $B_D = 2v\theta_a/\lambda$ where θ_a is the azimuth beamwidth of the antenna. At reasonable velocities, this value is on the order of a few hundred Hertz so that the minimum PRF as constrained by Δf_{min} is much higher than required by Nyquist.

While these high PRFs allow us to remove the feedthrough from the dechirped signal with a BPF, they also stretch out the spectrum of the radar returns, as differences in range now translate into much greater differences in frequency. The microASAR limits its range to echoes that are received within one tenth of the pulse repetition interval, which limits the bandwidth of the baseband dechirped signal to 12 MHz. According to the Nyquist constraint, it would be necessary to sample this data at 24 MHz in order to avoid aliasing. Assuming 16-bit samples, this would require storing raw data at a rate of 48 MBytes/sec.

We avoid extreme storage rate requirements by presumming the data before storing it. Let us assume, for instance, that our storage rate is limited to 5 MBytes/sec. If the system is operating at an altitude of 180 m and a velocity of 70 m/s, the minimum PRF as constrained by Δf_{min} is calculated to be $f_{p,min} = 7.8$ kHz. The Doppler bandwidth, as defined above, is $B_D = 389.1$ Hz which means that the minimum PRF to avoid Doppler aliasing is $2(389.1) = 778.2$ Hz. Presumming every 10 lines in the azimuth direction reduces the operating PRF of 7.8 kHz to an effective PRF of $f_{p,eff} = 780$ Hz, which still meets the constraints of the Doppler spectrum. Presumming reduces the amount of data that needs to be stored by a factor of 10. Thus we can now store the data at 4.8 MBytes/sec and still have sufficient information to reconstruct a high-quality image. As the PRF is lowered, the allowable presum factor must also be lowered, thus increasing the data rate. For this reason, the maximum data rate sets a lower bound on the PRF. In this example, the maximum storage rate of 5 MBytes/sec means that the PRF must be approximately 7.8 kHz or higher.

Using the method outlined above, the capabilities of the microASAR have been calculated over a range of different operating conditions. Calculated swath width versus altitude for a range of veloc-
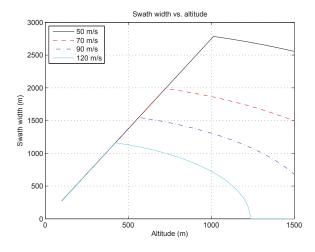
Fig. 3. Maximum swath width versus altitude for different velocities. The linear first portion of the plot is limited by an antenna 3 dB beamwidth of $50°$, the second portion is limited by a maximum storage rate of 5 MBytes/sec. The swath width may be increased by increasing the storage rate.

Table 1. microASAR System Specifications

Physical Specifications	
Transmit Power	30 dBm
Supply Power	< 35 W
Supply Voltage	+15 to +26 VDC
Dimensions	22.1x18.5x4.6 cm
Weight	3.3 kg
Radar Parameters	
Modulation Type	LFM-CW
Operating Frequency Band	C-band
Transmit Center Frequency	5428.76 MHz
Signal Bandwidth	80-160 MHz (variable)
PRF	7-14 kHz (variable)
Radar Operating Specifications	
Theoretical Resolution	1.25 m (@ 120 MHz BW)
Operating Altitude	100-1500 m
Max. Swath Width	300-2500 m (alt. dependent)
Operating Velocity	10-150 m/s
Collection Time (for 10GB)	30-60 min (PRF dependent)
Antennas (2 required)	
Type	2 x 8 Patch Array
Gain	15.5 dB
Beamwidth	$8.5°$x$50°$
Size	35x12x0.25 cm

ities is displayed in Fig. 3. These results are summarized in Table 1 along with system specifications.

3. MICROASAR HARDWARE

The microASAR is completely contained in one aluminum enclosure measuring 22.1x18.5x4.6 cm. The enclosure is designed to minimize spurious emissions, self-interference, and interference from outside sources. Despite its solid metal enclosure, the entire system, including two antennas, weighs less than 3.3 kilograms. Its lightweight design makes it suitable for aircraft with payload restrictions, such as UAVs.

A simplified block diagram showing the functions of the major signal paths is given in Fig. 2. To maintain phase coherence, all signals and clocks are derived from a single temperature compensated crystal oscillator (TCXO) which has been tuned specifically so that the feedthrough component can be removed as discussed in Section 2. The DDS generates the LFM chirp, which is then upconverted, amplified, and transmitted. A copy of this transmitted chirp is frequency-shifted and mixed with the received signal to produce the dechirped signal. The dechirped signal is then downconverted to an offset video frequency and sampled.

The digital subsystem for the microASAR contains the DDS chip which is used to generate the LFM chirp, a high-speed 500 Msps ADC, and a Virtex 4 FPGA. The FPGA is used to control the other chips, as well as to perform simple, pre-storage processing such as presumming and filtering. Because the dechirped radar data is sampled at an offset video frequency, it is necessary to filter and downsample in order to obtain baseband data for storage. A digital bandpass filter performs the dual task of reducing quantization noise and limiting the bandwidth of the dechirped signal so that it will not alias destructively. This filter/decimate operation is accomplished by way of a polyphase decimating filter. The decimation is designed so that an aliased copy of the signal ends up at baseband, eliminating the need for a separate mixing operation. After the data has been presummed, filtered, decimated, and low-pass filtered, the baseband signal is written to two flash memory cards, which are accessible through the front panel of the system.

4. CALCULATED SNR AND PROJECTED PERFORMANCE

Using the derivation in [4], we estimate the performance of the microASAR. The signal-to-noise ratio for a single radar pulse is

$$SNR_{sp} = \frac{P_r}{P_n} = \frac{P_t G^2 \lambda^2 \sigma^0 r_a r_y}{(4\pi)^3 R^4 k T_0 B F} \quad (4)$$

where P_r, P_n, and P_t are the power received, power from noise, and transmitted power; G is the antenna gain; λ is the transmit wavelength; r_a and r_y are along- and cross-track resolutions; σ^0 is the target radar cross section; R is range to target; k is Boltzmann's constant; $T_0 = 290K$ is the system noise temperature; B is the transmit signal bandwidth; and F is the receiver noise figure.

In order to account for the gain in SNR due to compression of the raw SAR data into an image, Eq. (4) is multiplied by

$$N_s = \frac{\lambda R}{2 r_a v T_p} \quad (5)$$

where v is the velocity of the platform and T_p is the pulse repetition interval. For LFM-CW SAR, $T_p = 1/f_p$. If presumming is being performed, the SNR is improved by a factor of approximately $\sqrt{M}$ where M is the number of lines averaged before azimuth processing [5]. In this case, T_p in Eq. (5) needs to be multiplied by the presum factor as well.

The SNR after compression is

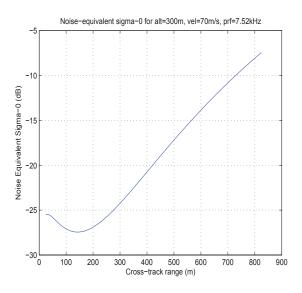$$SNR = \frac{P_r}{P_n} = \frac{P_t G^2 \lambda^3 \sigma^0 r_y \sqrt{M}}{2(4\pi)^3 R^3 k T_0 B F v T_p M} \quad (6)$$

V - 516

Fig. 4. Noise-equivalent σ^0 over expected cross-track range for the micro-ASAR with reasonable operating parameters.

Fig. 5. microASAR with cover removed showing RF components. Also pictured is the front panel containing RF ports, flash memory cards, serial and ethernet connections.

Using Eq. (6), noise-equivalent σ^0 values can be calculated for the microASAR operating at a variety of altitudes, velocities, and PRFs. A graph of noise-equivalent σ^0 versus cross-track range for reasonable operating parameters is displayed in Fig. 4. Targets with a σ^0 higher than the noise-equivalent σ^0 will be discernable above the noise-floor in the SAR image. The mid-range value of noise-equivalent σ^0 for the given altitude, velocity, and PRF is approximately -17 dB. This corresponds to desert terrain and dry, broken soil [4]. Vegetation and developed areas have higher values of σ^0 and will show up even more brightly. The SNR can be improved by lowering the operating altitude or increasing the PRF, although both changes result in a narrower image swath. It is also possible to improve the SNR by adding an external power amplifier for the transmitted signal. It should be noted that, because of the small antennas, the azimuth resolution of the microASAR is much finer than the range resolution. This is generally accounted for by performing multi-look averaging on the final image so that each resolution cell is approximately square. Like presumming, this operation produces an SNR gain proportional to $\sqrt{L}$ where L is the number of azimuth lines averaged [5]. For the microASAR, this results in a 2-3 dB SNR gain over the results in Fig. 4.

5. CONCLUSION

The microASAR is a highly capable SAR system that is specifically designed for applications that require a small, lightweight, low-power solution. This paper has outlined the general methodology used in designing the system and has described the hardware specifications. Results from SNR calculations are presented and system performance predicted.

LFM-CW operation requires less power than a comparable pulsed SAR and enables hardware which is less complicated, and thus easier to fabricate. The hardware solution provided by Artemis, Inc., (shown in Fig. 5), is robust enough to withstand the rigors of airborne applications while still being small and lightweight. The system provides an accessible option for high-quality SAR imagery which will be useful for area studies.

6. REFERENCES

[1] E.C. Zaugg, D.L. Hudson, and D.G. Long, "The BYU μSAR: A small, student-built SAR for UAV operation," in *Proc. Int. Geosci. Rem. Sen. Symp.*, Denver, Colorado, Aug. 2006, pp. 411–414.

[2] M.I. Duersch, "BYU micro-SAR: A very small, low-power, LFM-CW synthetic aperture radar," Master's Thesis, Brigham Young University, Provo, Utah, 2004.

[3] D.G. Thompson, D.V. Arnold, and D.G. Long, "YINSAR: a compact low-cost interferometric synthetic aperture radar," in *Proc. Int. Geosci. Rem. Sen. Symp.*, Hamburg, Germany, July 1999, pp. 598–600.

[4] F. T. Ulaby, R. K. Moore, and A. K. Fung, *Microwave Remote Sensing: Active and Passive*, vol. 2, Addison-Wesley, Reading, MA, 1981.

[5] J. C. Curlander and R. N. McDonough, *Synthetic Aperture Radar: Systems and Signal Processing*, pp. 220–221, Wiley, New York, NY, 1991.